

# Characterization of ZnO:Si Nanocomposite Films Grown by Thermal Evaporation.

Shabnam Siddiqui and Chhaya Ravi Kant

*Department of Applied Sciences, Indira Gandhi Institute of Technology,  
Guru Gobind Singh Indraprastha University, Delhi 110 006, India.\**

P. Arun

*Department of Physics & Electronics, S.G.T.B. Khalsa College,  
University of Delhi, Delhi - 110 007, India<sup>†</sup>*

N.C.Mehra

*University Science Instrumentation Centre,  
University of Delhi, Delhi 110 007, India.*

## Abstract

Nanocomposite thin films of Zinc Oxide and Silicon were grown by co-evaporating powdered ZnO and Si. This resulted in nanocrystallites of ZnO being embedded in Silicon. The mismatch in crystal structures of constituent materials result in the ZnO nanocrystals to exist in a state of stress. This along with oxygen vacancies in the samples result in good Photoluminescence emission at 520nm. Also, Silicon background gave a photoluminescence emission at 620nm. The structure was found quite stable over time since the homgenously dispersed ZnO nanocrystals do not agglomerate. The nanocomposites promises to be a useful candidate for future optoelectronic devices.

PACS numbers: 81.07.Bc, 81.07.Ta, 78.67.Hc, 07.79.Lh, 78.55.-m

## I. INTRODUCTION

Since the fabrication of blue wavelength LED in the last decade, research has gone on to attain LEDs of all possible wavelengths, even in the Ultra Violet wavelength range. Nanotechnology presents a possible method of achieving this objectivity. It has been observed that in the nanometer regime, the band gap of a semiconducting material increases with reduction of its particle/ grain size.<sup>1</sup> This presents a possibility of manufacturing materials of any desirable optical and electronic properties. However a problem confronted is that materials existing as nanoparticles tend to agglomerate, giving particles of larger size.<sup>2</sup> To prevent further growth of particles capping agents were added during fabrication. This method has been extensively used in liquid phase. Alternatively, especially in the solid phase, nanoparticles have been grown embedded in a featureless background which is unmarked as far as its properties are concerned in region of interest for that of the nanoparticles.

Researchers working to develop LEDs/lasers which emit light with low wavelengths show immense interest in ZnO since it exhibits quantum confinement effects in the experimentally accessible range of sizes. Also, it helps that ZnO is a wide band gap semiconductor materials, with possible application not only in electro-optical devices but also as varistors and transparent conducting films. ZnO nanoparticles also exist in various morphological states like nanowires, nanorods, nanospheres etc.<sup>3,4,5,6,7,8,9,10,11,12,13,14,15,16</sup> This presents rich information from a pure science point of view for understanding the basic quantum mechanical behaviour of matter in nanostate.

Various processing techniques have been tried and developed to manufacture nano-sized samples in a controlled fashion. Of the many methods, a recent attempt by Singh et al<sup>17</sup> attracted our attention, where the size of nanocrystalline ZnO was controlled by growing them on porous-silicon substrates, whose pore size was controllable. Though their results were interesting, the fabrication process was involved and in our opinion not commercially viable. We decided to investigate a possible process where nanocomposites of zinc oxide and silicon could be fabricated without the tedious process reported<sup>17</sup> yet present features similar to those reported in the above mentioned study. In this article we report our observations

on nanocomposites obtained by thermal co-evaporation of silicon and zinc oxide.

## II. EXPERIMENTAL DETAILS

ZnO:Si nanocomposite films were grown by thermal evaporation method using JEOL, JEE 4X vacuum evaporation unit. n-Si wafers were ground into powder and to this powder ZnO was added in a proportion of 2:1. The two were mixed by grinding in an agate. Powdered ZnO of high purity (99.99%) was obtained from Merck (Mumbai). Such well mixed material was then palletized to be used as the starting material. The nanocomposite films were grown on microscopic glass substrates held at room temperature. The films were grown at vacuum better than  $10^{-6}$ - $10^{-7}$ Torr. The structural studies of the films were done using X-ray diffractometer (Philips PW 3020). The film's surface morphology and texture were studied using the Scanning Electron Microscope (SEM) JEOL (JSM)-840 Scanning Microscope. Raman Spectra and Photoluminescence were recorded using Renishaw's "*Invia Reflex*" Raman Spectroscopy and Shimadzu's PL Spectroscopy respectively.

## III. RESULTS AND DISCUSSIONS

Films of various thickness were fabricated and studied. Of all the samples studied, we report and compare the results of three extreme thicknesses here (in accordance of thickness  $G1 < G3 < G2$ ).

### A. X-Ray Diffraction & Morphological Studies

As grown sample of G1 show a lone peak at  $2\theta = 36.895^\circ$  (fig 1). JCPDS card (No. 36-1451) reports this as the (101) peak of ZnO. This corresponds to the wurtzite structure that bulk ZnO is known to crystallize in with lattice constants  $a \sim 0.3250\text{nm}$  and  $c \sim 0.5207\text{nm}$ . The XRD peaks are considerably broadened and are indicative of very small size particles and in turn existence of nanocrystals. The average crystallite size of the particles in the film

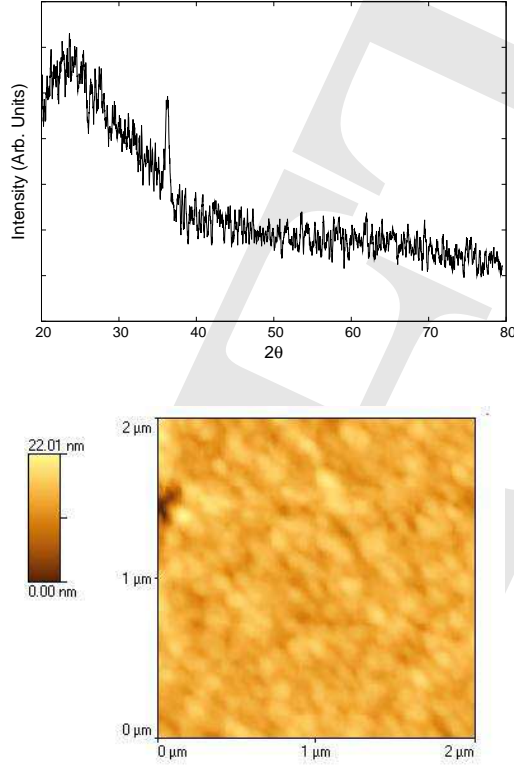


FIG. 1: The X-Ray diffractogram of as-grown nanocomposite thin film (G1) along with its AFM image.

can be calculated by Scherrer's formula.

$$D = \frac{0.9\lambda}{B\cos\theta} \quad (1)$$

where  $D$  is the grain size (in  $\text{\AA}$ ),  $B$  is the FWHM of the particular peak in radians,  $\theta$  is the Bragg's angle and  $\lambda$  ( $\sim 1.5405\text{\AA}$ ) is the wave-length of X-ray. The size of the grains in the as-grown sample of G1 was computed to be 20nm. The hump seen in the X-ray diffractogram show the short range ordering of silicon atoms in the background. Such hump has been observed in amorphous silicon studied by Gwo-Mei et al<sup>18</sup>. While the X-Ray diffraction pattern prove the existence of nanocrystallinity, a direct verification of their

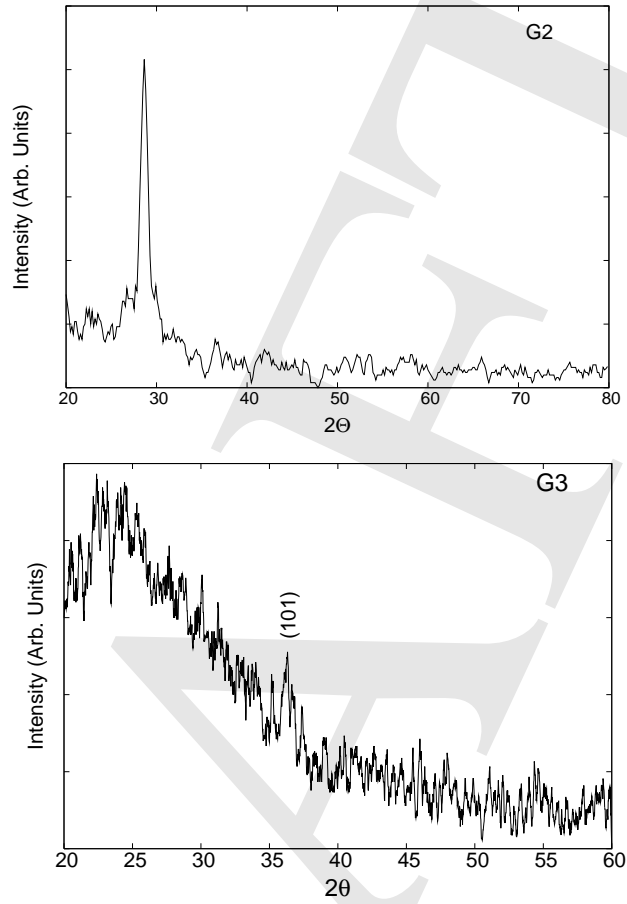


FIG. 2: X-Ray diffractograms of asgrown nanocomposite thin films, G2 and G3. On comparing with the diffractogram of G1 shown in fig 1, it is clear that the lone peak of ZnO diminishing with increasing film thickness.

existence and the particle size can be done by examining them with electron microscope (results not shown here) or for more localised areas using the Atomic Force Microscope (AFM). The average grain size as measured from the AFM image was  $\sim 100\text{nm}$  (fig 1). The disagreement between the results from the diffractograms and AFM images implies that the diffraction peak's broadening is not just due to the grain sizes. X-Ray peaks are known to become broad due to the existence of stress/ defects in the crystal.<sup>19</sup> Thus, we expect the nanocrystals of ZnO formed in the film to be in a stressed state with defects in the crystal

structure. Such observations of stress in ZnO films grown on silicon substrates have been reported and explained on the basis of large mismatch between the two material's lattice constants.<sup>20</sup> The stressed condition are expected to manifest itself in the optical properties of the samples.

The asgrown films of G2 too show a lone peak, however at  $2\theta = 28.485^\circ$ . This is the characteristic (111) peak of silicon. The average size of silicon grains in our G2 asgrown sample as calculated using the Scherrer's formula was found to be 10nm. It can be noticed that as the film thickness increases, the nanocrystallinity of ZnO is screened by the increasing ordering of silicon (fig 2). This is unlike in G1 where a well resolved peak of ZnO stands out compared to the short range ordering of silicon. With increasing thickness of the film the ordering of silicon atoms improves and the hump corresponding to short range order gives way to a peak. Peaks of Zinc oxide are not evident, however nanocrystals of ZnO can not be ruled out. It was not possible to resolve whether two distinct morphologies exist from the AFM images (not included). Evidence for the coexistence of two nanocrystals however was resolved from our optical characterisations.

## B. Optical Studies

Raman scattering was performed to investigate the vibrational properties of the ZnO nanocrystals and Si in which the nanocrystals are embedded. The Raman spectra was taken in standard back scattering geometry with  $\text{Ag}^{2+}$  laser used as an excitation source. Vibrational spectra from ZnO nanocrystals, silicon background and the glass substrate can be expected. However, silicon oxide has no contribution to Raman spectrum.<sup>21</sup> Hence contributions from the glass substrate can be ruled out. The Raman spectra of ZnO has been well documented and reported to have both longitudinal optical (LO) and transverse optical (TO) phonon frequencies that split into two frequencies with symmetries  $A_1$  and  $E_1$ .<sup>22</sup> Prominent among the peaks is the  $A_1(\text{LO})$  mode vibration of ZnO at  $570\text{cm}^{-1}$ . Other important Raman peaks of zinc oxide are the  $E_2$  intense peak at  $438\text{cm}^{-1}$  and the weak  $E_1(\text{LO})$  peak at  $585\text{cm}^{-1}$ . Since this peak ( $585\text{cm}^{-1}$ ) is very close to the  $A_1(\text{LO})$  peak ( $570\text{cm}^{-1}$ ),

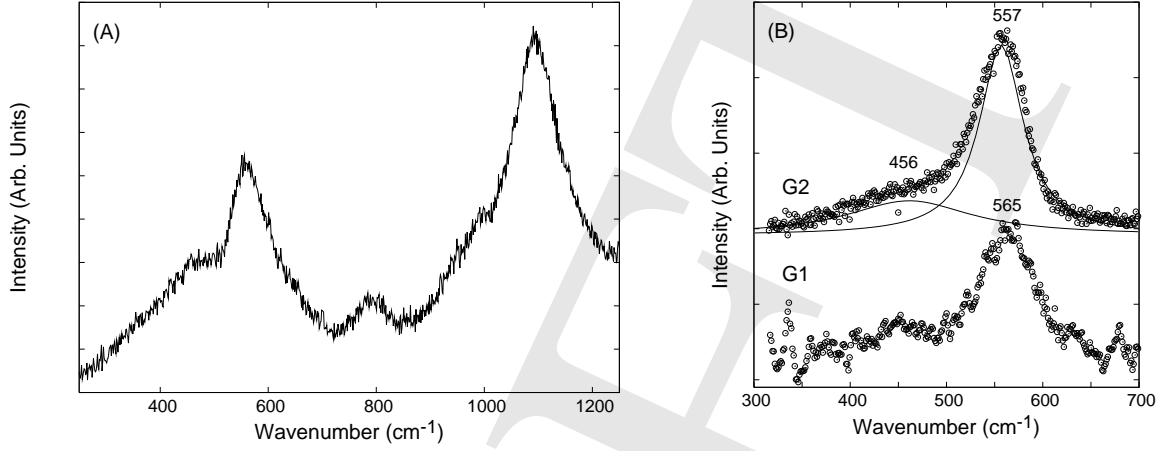


FIG. 3: The Raman spectra of (A) G1 sample and (B) compares spectra of G1 and G2 sample in range  $300\text{-}700\text{cm}^{-1}$ .

both usually result in an apparent single broad peak. Along with these major peaks, two weak peaks at  $332\text{cm}^{-1}$  and  $381\text{cm}^{-1}$  have been reported.<sup>16</sup>

Besides these vibrational peaks, a prominent LO mode is expected around  $1100\text{-}1150\text{cm}^{-1}$ .<sup>23,24,25,26</sup> The position of this peak in G1 is at  $1095\text{cm}^{-1}$  (fig 3A). Peak width and shifts indicates the size of the nano-crystals. As the crystallite size increases the peaks becomes broader and shifts to lower energy.<sup>27,28,29,30</sup> Thus our films contain small sized nanoparticles of ZnO. Other observed peak associated with zinc oxide was the  $E_1(\text{LO})$  mode at  $585\text{cm}^{-1}$ . However, prominent by it's omission is the  $E_2$  peak around  $438\text{cm}^{-1}$ . This peak is associated with the wurtzite crystal structure of zinc oxide. The absence of intense Raman-active mode at  $438\text{cm}^{-1}$  and existence of peak at  $585\text{cm}^{-1}$  in our samples corroborate our X-Ray diffraction results that our samples have possible structural defects like oxygen vacancies, zinc interstitials and free carriers etc.<sup>5</sup>

Zinc oxide nanocrystals of sample G1 and G3 are embedded in a matrix background of amorphous silicon. The Raman spectrum of amorphous Silicon (a-Si) consists of several broad bands, the transverse acoustic (TA) is found at  $150\text{cm}^{-1}$  and the longitudinal acoustic band (LA) at  $310\text{cm}^{-1}$ . As expected a sharp peak that can be ascribed to a-Si can be seen  $\sim 300\text{cm}^{-1}$ . X-Ray diffraction results suggested the background of G2 samples

to consist nanocrystalline Silicon (n-Si). Evidence of this was also found in our Raman studies. The spectrum of n-Si is very similar to that of the single crystal silicon (c-Si) with a peak appearing at  $519.4\text{cm}^{-1}$ . However, additional peaks appear at  $604$  and  $423\text{cm}^{-1}$  in n-Si samples.<sup>31</sup> As a result we expect a broadening and existence of a multi-peak band between  $400$  and  $600\text{cm}^{-1}$ . Comparing the Raman spectra of G2 and G1 between these two wavenumbers (fig 3B), we can appreciate the broadening that takes place in sample G2. A deconvolution was performed on the Raman spectra of G2 by assuming the peaks to have Lorentzian shapes. The peak shown at  $456\text{cm}^{-1}$  couldn't be deconvoluted further due to the lack of prominent shoulders in the spectra, but it should be a multi-peak band comprising the  $423\text{cm}^{-1}$  peak of n-Si and  $438\text{cm}^{-1}$  peak of ZnO. The confidence with which deconvolution can be done using standard softwares like Origin6.0 depends on the shoulders present in unresolved peaks. Since, we did not have many shoulders, we did not try to force more than two peaks for deconvolution.

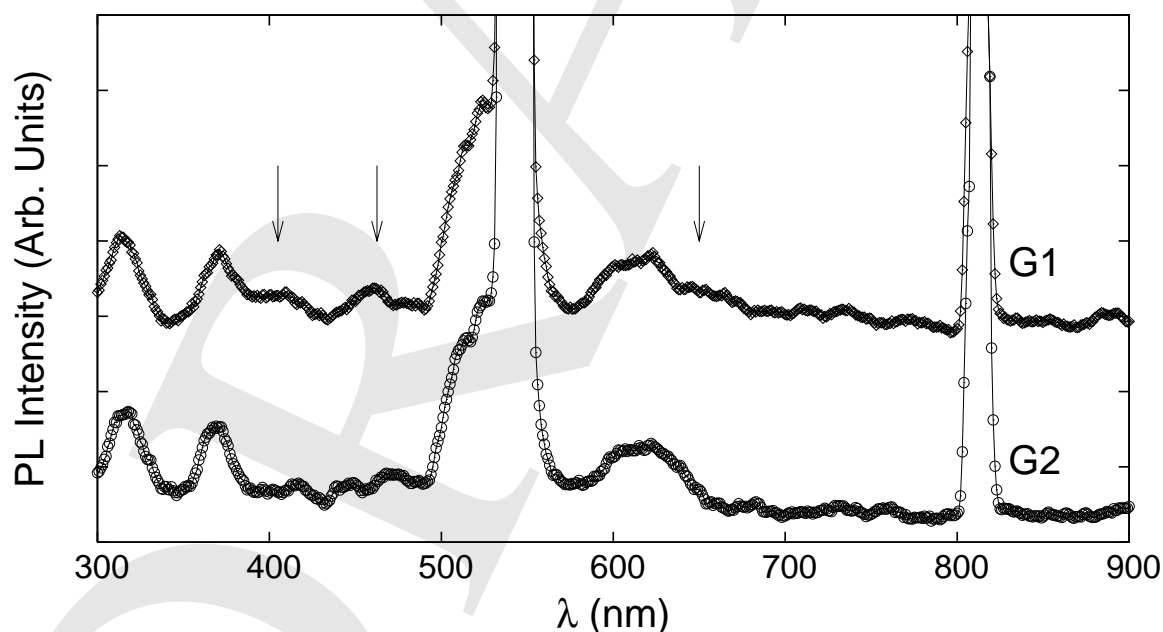


FIG. 4: The PL spectra of G1 and G2 asgrown samples. The spectra are near identical with peak broadening (indicated by arrows) in G1 sample, where ZnO nanocrystals are embedded in a-Si.

The results from Raman spectra analysis reinforces our conclusions made from structural

and morphological studies and confirm the formation of ZnO quantum dots in a matrix amorphous background of silicon in samples G1 and G3. In sample G2, the quantum dots of ZnO are suspended in a matrix of nanoparticles of silicon. Zinc oxide in the nano regime exhibits strong photoluminescence, hence a direct proof of the existence of ZnO in nanocrystalline state can be obtained from the PL peaks. As stated above, the peak at  $570\text{cm}^{-1}$  in Raman spectra originates due to structural defects (oxygen vacancies, zinc interstitials and/or free carriers etc.) and impurities.<sup>5</sup> It has been reported that such structural defects in ZnO nanocrystals give rise to new peaks in PL spectra.

The photoluminescence (PL) spectrum for the G1 and G2 samples are shown in Fig 4. The emission spectra were obtained using 270nm excitation source. The spectra were recorded without filters and hence we see two lines, the 2<sup>nd</sup> and 3<sup>rd</sup> harmonics of the source at 540 and 810nm respectively. Characteristic peaks of ZnO and Si are observed at 310nm, 365nm, 522nm and 620nm. ZnO nanoparticles giving PL emissions in the UV region have been reported<sup>32,33</sup> and have been explained due to the radiative annihilation of excitons. The position of the green emission peak ( $\sim 520\text{nm}$ ) was resolved by deconvoluting the emission peak and 2<sup>nd</sup> harmonic line spectra (see fig 5). The peak position is in good agreement with earlier reports.<sup>34,35</sup> The green emission of ZnO nanocrystals are explained due to transition of electrons from the conduction band to trapped hole within the band gap. Oxygen vacancies, in other words defects, are considered to be the main candidate for recombination centers involved in this emission.<sup>36,37</sup> Our XRD analysis with peak broadening suggested that our samples had defects. Defects were also indicated by our Raman spectra. This is confirmed by the green emission band in PL studies. The 620nm emission spectra belongs to the silicon matrix of our samples.<sup>38</sup>

The PL emission spectra (fig 4) of G1 and G2 samples appear identical. While G1 sample had ZnO nanocrystals embedded in a matrix of amorphous silicon, ZnO nanocrystals of G2 sample are embedded in nanocrystalline silicon. The only variation due to the structurally different matrix (background) seems to be the disappears of shoulders in peaks (indicated by pointers in fig 4) as silicon goes from amorphous to nano-crystalline state. While this geometry has not given multiple emission peaks in visible region (unlike case reported where

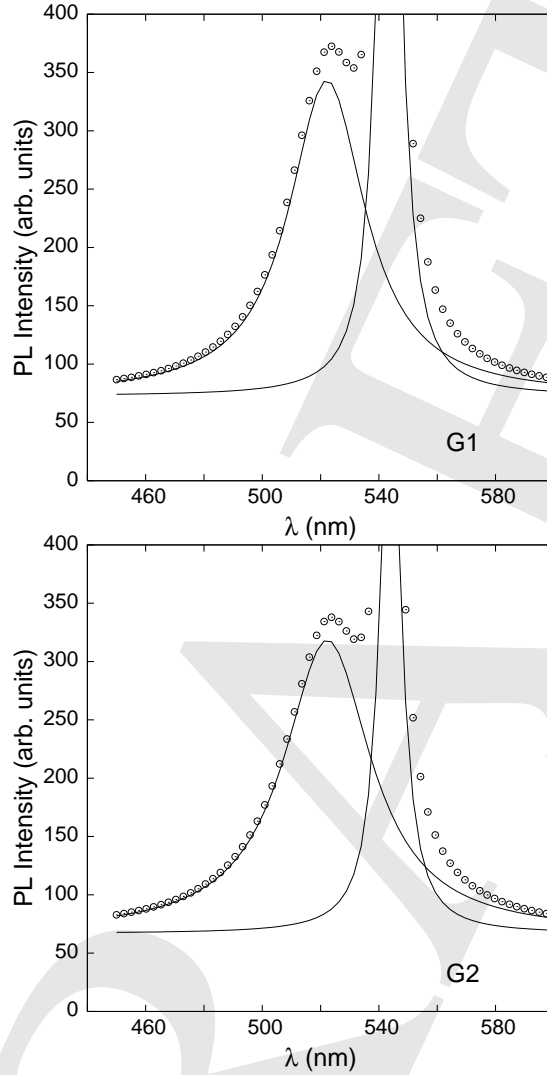


FIG. 5: The green band in PL spectra was deconvoluted to resolve the emission peak from the intense 2<sup>nd</sup> harmonic peak of the 270nm excitation source.

ZnO was grown on porous-silicon substrate<sup>17</sup>) it has given stability to the ZnO nanocrystals. The PL spectra has maintained its nature over 90 days since sample fabrication. Also, the strength of emission in our samples is far stronger than that observed in samples of Singh et al.<sup>17</sup> We believe the thermal evaporation method used for sample fabrication leads to the nanocrystals of ZnO to be homogeneously enveloped by silicon, thus contributing to the strong emission spectra. Thus, this method of fabrication might result in more efficient

opto-electronic devices designed around the feature of green emission.

If the emission peak due to silicon at 620nm can be made strong and intense, it would merge with the peak due to ZnO at 520nm and result in a broad-band spectra. We believe that strong broad band emission can be obtained by the simple fabrication method we have adopted. In order to obtain this, the parameters such as film thickness, substrate temperature, amount of ZnO dispersed in Si matrix and the other deposition conditions have to be optimized. Such studies are being done by our group.

#### IV. CONCLUSION

ZnO:Si nanocomposites were fabricated by co-thermal evaporation of ZnO and Si powder. Resulting films yielded nanocrystalline ZnO embedded in amorphous Silicon or nanocrystalline Silicon, depending on the film thickness. The PL emission spectra of these films present two neighboring emission peaks at 520 and 620nm due to ZnO nanocrystals and silicon respectively. On optimization, broad-band emission could eventually result white light emission. The method holds promise as potential low-cost fabrication method for white LEDs etc.

#### Acknowledgment

The resources utilized at University Science and Instrumentation Center, University of Delhi and Geology Department, University of Delhi is gratefully acknowledged. Also, the resources used at the Instrumentation Center and University Information Resource Center, Guru Gobind Singh Indraprasta University is also acknowledged. We also would like to express our gratitude to Mr. Kamal Saran (National Physical Lab., Delhi) for carrying out the photoluminescence studies.

---

\* Electronic address: [chhaya.rkant@yahoo.co.in](mailto:chhaya.rkant@yahoo.co.in)

- † Electronic address: arunp92@physics.du.ac.in, arunp92@yahoo.co.in
- <sup>1</sup> A. D. Yoffe, *Adv. Phys.*, **51** (2002) 799.
  - <sup>2</sup> “Nanoparticles: From Theory to Application”, ed Gunter Schmid (Wiley-VCH, Weinheim, 2004).
  - <sup>3</sup> A. Sekar, S.H. Kim, A. Umar, Y.B. Hahn, *J. Cryst. Growth* **277** (2005) 471.
  - <sup>4</sup> A. Umar, H.W. Ra, J.P. Jeong, E.-K. Suh, Y.B. Hahn, *Korean J. Chem. Eng.* **23** (2006) 499.
  - <sup>5</sup> A. Umar, S.H. Kim, Y.S. Lee, K.S. Nahm, Y.B. Hahn, *J. Cryst. Growth* **282** (2005) 131.
  - <sup>6</sup> A. Umar, B. Karunagaran, E.-K. Suh, Y.B. Hahn, *Nanotechnology* **17** (2006) 4072.
  - <sup>7</sup> W.L. Hughes, Z.L. Wang, *Appl. Phys. Lett.* **82** (2003) 2886.
  - <sup>8</sup> B.P. Zhang, N.T. Binh, K.Wakatsuki, Y. Segawa, Y. Yamada, N. Usami, H. Koinuma, *Appl. Phys. Lett.* **84** (2004) 4098.
  - <sup>9</sup> A. Umar, Y.B. Hahn, *Appl. Phys. Lett.* **88** (2006) 173120.
  - <sup>10</sup> W.L. Hughes, Z.L. Wang, *J. Am. Chem. Soc.* **126** (2004) 6703.
  - <sup>11</sup> P.X. Gao, Z.L. Wang, *J. Appl. Phys.* **97** (2005) 44304.
  - <sup>12</sup> A. Umar, S. Lee, Y.S. Lee, K.S. Nahm, Y.B. Hahn, *J. Cryst. Growth* **277** (2005) 479.
  - <sup>13</sup> A. Umar, S. Lee, Y.H. Im, Y.B. Hahn, *Nanotechnology* **16** (2005) 2462.
  - <sup>14</sup> A. Umar, S.H. Kim, Y.H. Im, Y.B. Hahn, *Superlattices Microstruct.* **39** (2006) 238.
  - <sup>15</sup> G. Shen, Y. Bando, B. Liu, D. Golberg, C.J. Lee, *Adv. Func. Mater.* **16** (2006) 410.
  - <sup>16</sup> A. Umar, Y.B. Hahn, *Nanotechnology* **17** (2006) 2174.
  - <sup>17</sup> R. G. Singh, Fouran Singh, V. Aggarwal and R. M. Mehra, *J. Phys. D: Appl. Phys.* **40** (2007) 3090.
  - <sup>18</sup> Gwo-Mei Wu and Chen-Yen Wu, *Cryst. Res. Technol.* **42** (2007) 1271.
  - <sup>19</sup> G. C. Badakoti, B. Kumar, G. Bhagavannarayana and N. C. Soni, *Phys. Stat. Sol. (a)*, **202** (2005) R7.
  - <sup>20</sup> H-C Hsu, C-S Cheng, C-C Chang, S. Yang, C-S Chang and W-F Hseih, *Nanotechnology*, **16** (2005) 297.
  - <sup>21</sup> Jianxun Liu, Junjie Niu, Deren Yang, Mi Yan, Jian Sha, *Physica E* **23** (2004) 221.

- <sup>22</sup> J.M. Calleja, M. Cardona, Phys. Rev., B 160 (1977) 3753.
- <sup>23</sup> X.T. Zhang, Y.C. Liu, Z.Z. Zhi, J.Y. Zhang, Y.M. Lu, D.Z. Shen, W. Xu, G.Z. Zhong, X.W. Fan, X.G. Kong, J. Phys. D: Appl. Phys. **34** (2001) 3430.
- <sup>24</sup> J.F. Scott, Phys. Rev. B 2 (1970) 1209.
- <sup>25</sup> C. Roy, S. Byrne, E. McGlynn, J. P. Mosnier, E. de Posada, D. O'Mahony, J. G. Lunney, M. O. Henry, B. Ryan and A. A. Cafolla, Thin Solid Films, **436** (2003) 273.
- <sup>26</sup> A. Goldenblum, A. Belu Marian and V. Teodorescu, J. Optoelect. Adv. Mater., **8** (2006) 2129.
- <sup>27</sup> M. Rajalakshmi, A. K. Arora, B. S. Bendre, and S. Mahamuni, J. Appl. Phys. **87** (2000) 2445.
- <sup>28</sup> C. L. Yang, J. N. Wang, W. K. Ge, L. Guo, S. H. Yang, and D. Z. Shen, J. Appl. Phys. **90** (2001) 4489.
- <sup>29</sup> L. Guo, S. Yang, C. Yang, P. Yu, J. Wang, W. Ge, and G. K. L. Wong, Appl. Phys. Lett. **76** (2000) 2901.
- <sup>30</sup> K. A. Alim, V. A. Fonoberov, and A. A. Balandin, Appl. Phys. Lett. **86** (2005) 053103.
- <sup>31</sup> Z. Iqbal, S. Veperk, J. Phys. C **15** (1982) 377.
- <sup>32</sup> Eva M. Wong and Peter C. Searson, Appl. Phys. Lett., **74** (1999) 2939-2941.
- <sup>33</sup> CongKang Xu, Misuk Kim, Sangyong Chung and Dong-Eon Kim, Solid State Comm., **132** (2004) 837-840.
- <sup>34</sup> K. Vanheusden, W.L.Warren, C.H.Seager, D.R. Tallant, J.A.Voigt and B.E. Gnade, J. Appl. Phys., **79** (1996) 7983.
- <sup>35</sup> U.V. Siva Kumar, F. Singh, AMit Kumar, D.K. Avasthi, Nucl. Instr. Meth. Phys. Res. B, **244** (2006) 91-94.
- <sup>36</sup> A. van Dijken, E.A. Meulenkaamp and D. Vanmaekelbergh, J. Lumin., **90**, (2000) 123.
- <sup>37</sup> A. van Dijken, E.A. Meulenkaamp and D. Vanmaekelbergh, J. Phys. Chem. B, **104**, (2000) 1715.
- <sup>38</sup> S. Tripathy, R.K. Soni, S.K. Ghoshal and K.P. Jain, Bull. Mater. Sci., **24** (2001) 285-289.